

Electronic Supplementary Information

Solvent-modulated metamagnetism in a nickel(II) coordination polymer with mixed azide and carboxylate bridges

Wei-Wei Sun, Chun-Yan Tian, Xue-Hui Jing, Yan-Qin Wang and En-Qing Gao*

Syntheses and general characterization: A mixture of 1-carboxymethylpyridinium-4-acrylic acid (0.021 g, 0.10 mmol), NiCl₂·6H₂O (0.024 g, 0.10 mmol), NaN₃ (0.026 g, 0.40 mmol), ethanol (1.0 mL) and H₂O (2.0ml) was sealed in a Teflon-lined autoclave and heated at 70 °C for 3 days, then cooled to room temperature at the speed of 5°C/h to give the green block crystals of **1** (yield 65% based on NiCl₂·6H₂O). IR (KBr, cm⁻¹) for **1**: 3530m, 3348br, 2084vs, 2059vs, 1650s, 1627vs, 1582s, 1505m, 1461w, 1388vs, 1307m, 985m. Anal. calcd. for C₂₀H₃₀N₁₄Ni₃O₁₅ (%): C, 27.22; N, 22.22; H, 3.43. Found (%): C, 27.11; N, 22.50; H, 3.82. The bulk phase purity of the sample has been confirmed by powder X-ray diffraction (PXRD) measurements, which give a pattern agreeable with that calculated from the single-crystal data (Fig. S4).

Thermogravimetric analysis (TGA) reveals two dehydration steps (Fig. S5). The first step occurs from 35 to 65 °C with a weight loss of about 9.1%, assignable to the loss of the uncoordinated water molecules (calcd. weight loss, 10.2 %). The second step is between 120 and 145°C, the weight loss (3.0%) corresponding to the loss of the coordinated water molecules (calcd. weight loss, 4.0 %). The framework decomposition occurs above 220 °C. Thus the fully dehydrated material **2** was obtained by heating the crystals of **1** at 140 °C in vacuum for two hours. IR (KBr, cm⁻¹) for **2**: 2096vs, 2057vs, 1640vs, 1582s, 1503m, 1384vs, 1300m, 985m. Anal. calcd. for C₂₀H₁₆N₁₄Ni₃O₈ (%): C, 31.75; N, 25.92; H, 2.13. Found (%): C, 31.43; N, 25.97; H, 2.62. The complete dehydration is accompanied by a colour change from green to yellow green. The solid-state UV-visible spectrum of **1** (Fig. S6) shows *d-d* transition bands centered around 420 nm [³A_{2g} → ³T_{1g}(P)] and 685 nm [³A_{2g} → ³T_{1g}(F)], while the spectrum of **2** shows red shifts of about 40 nm, suggesting the weakening of the ligand field around Ni(II) upon dehydration. Powder X-ray diffraction (PXRD) analyses suggest that **2** is new crystalline phase different from **1**.[†] After **2** was exposed

to moist atmosphere (i.e., put the small tube containing the sample in a sealed vessel containing water), the green colour can be fully recovered and PXRD analyses suggested that the phase of **1** is also recovered (Fig. S4). The rehydration time may be several hours to a couple of days, depending upon the humidity of the atmosphere (controlled by temperature). Typically, the rehydration can be completed in four hours at 50 °C.

The partially dehydrated material **1'** was obtained by heating the crystals of **1** at 65 °C in air for three hours. The sample is still green in colour, but lighter than **1**. The UV-visible spectrum of **1'** (Fig. S6) is very similar to that for **1**, without appreciable shifts in *d-d* transition absorption maxima, suggesting that the coordination environment does not change much. IR (KBr, cm⁻¹) for **1'**: 3423br, 2150s, 2075vs, 1652s, 1645s, 1576m, 1560s, 1540s, 1513m, 1394vs, 1300m, 980m. PXRD analyses suggest that **1'** is a phase different from both **1** and **2** (Fig. S4) and can readily recover to **1** when exposed to moist atmosphere.

Crystal Data Collection and Refinement Diffraction intensity data were collected at 293 K on a Bruker APEX II diffractometer equipped with a CCD area detector and graphite-monochromated Mo K α radiation ($\lambda = 0.71073$ Å). Empirical absorption corrections were applied using the SADABS program.¹ The structures were solved by the direct method and refined by the full-matrix least-squares method on F^2 using the SHELXL program,² with anisotropic displacement parameters for all non-hydrogen atoms. The hydrogen atoms attached to carbon atoms were placed in calculated positions and refined using the riding model. The water hydrogen atoms attached to O5, O6 and O7 were located from the difference Fourier map and refined with restrained O-H and H...H distances (9 restraints using the DFIX instruction). The hydrogen atoms of the disordered water molecules could not be located. The O8 and O8' disordered water molecules were constrained to have the same anisotropic displacement parameters, and the occupancies were refined to be 0.37 and 0.13, respectively.

Analyses of the temperature-variable magnetic susceptibility. The experimental data were analyzed using the following expression derived by Escuer et al³ from the spin Hamiltonian $H = -J_1 \sum (S_{3i} S_{3i+1} + S_{3i+1} S_{3i+2}) - J_2 \sum S_{3i-1} S_{3i}$ in the classical-spin approximation.

$$\chi_{\text{chain}} = [Ng^2\beta^2 S(S+1)/(3kT)](A/B)$$

$$\text{with } A = 3(1 - u_1^4 u_2^2) + 4u_1(1 - u_1^2 u_2^2) + 2u_2(1 + u_1)^2(1 - u_1^2) + 2u_1^2(1 - u_2^2)$$

$$B = (1 - u_1^2 u_2)^2$$

$$u_i = \coth[J_i S(S+1)/kT] - kT/[J_i S(S+1)] \quad (i = 1, 2)$$

J_1 and J_2 are the intrachain coupling parameters defined in Fig. S1. To include the interchain magnetic interactions (zJ'), the molecular-field approximation was applied:⁴

$$\chi = \chi_{\text{chain}} / [1 - (zJ'/Ng^2\beta^2)\chi_{\text{chain}}]$$

For the convenience of comparison, the data of **1**, **1'** and **2** were all simulated in the temperature range 20-300 K, in which the fits of the three datasets using the same expression are all satisfactory (Fig. S7, bottom). The best-fit parameters are $J_1 = 21.7 \text{ cm}^{-1}$, $J_2 = 78.6 \text{ cm}^{-1}$ and $g = 2.17$ with $zJ' = -0.37 \text{ cm}^{-1}$ for **1**; $J_1 = 21.4 \text{ cm}^{-1}$, $J_2 = 79.9 \text{ cm}^{-1}$ and $g = 2.18$ with $zJ' = -0.46 \text{ cm}^{-1}$ for **1'**, $J_1 = 23.4 \text{ cm}^{-1}$, $J_2 = 72.2 \text{ cm}^{-1}$ and $g = 2.17$ with $zJ' = -0.77 \text{ cm}^{-1}$ for **2**. It should be noted these values are only rough approximations because the $S = 1$ spin for Ni(II) is far from a classical spin. Nevertheless, the relative values should reflect the real trends. The above results reveal similar intrachain ferromagnetic interactions and increased interchain antiferromagnetic interactions upon dehydration.

References

- 1 G. M. Sheldrick, *Program for Empirical Absorption Correction of Area Detector Data*; University of Göttingen, Germany, 1996.
- 2 G. M. Sheldrick, *SHELXTL* Version 5.1. Bruker Analytical X-ray Instruments Inc., Madison, Wisconsin, USA, 1998.
- 3 M. A. M. Abu-Youssef, M. Drillon, A. Escuer, M. A. S. Goher, F. A. Mautner, R. Vicente, *Inorg. Chem.* 2000, **39**, 5022.
- 4 R. L. Carlin, *Magnetochemistry*, Springer, Berlin-Heidelberg, 1986.

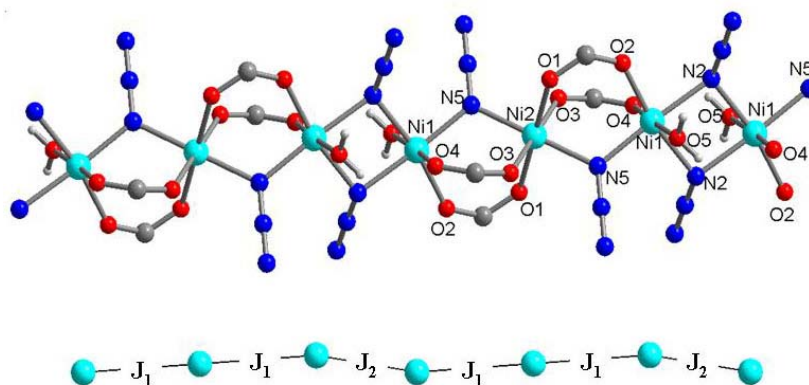


Fig. S1. Views showing the alternating bridges and exchange parameters along the chain in **1**.

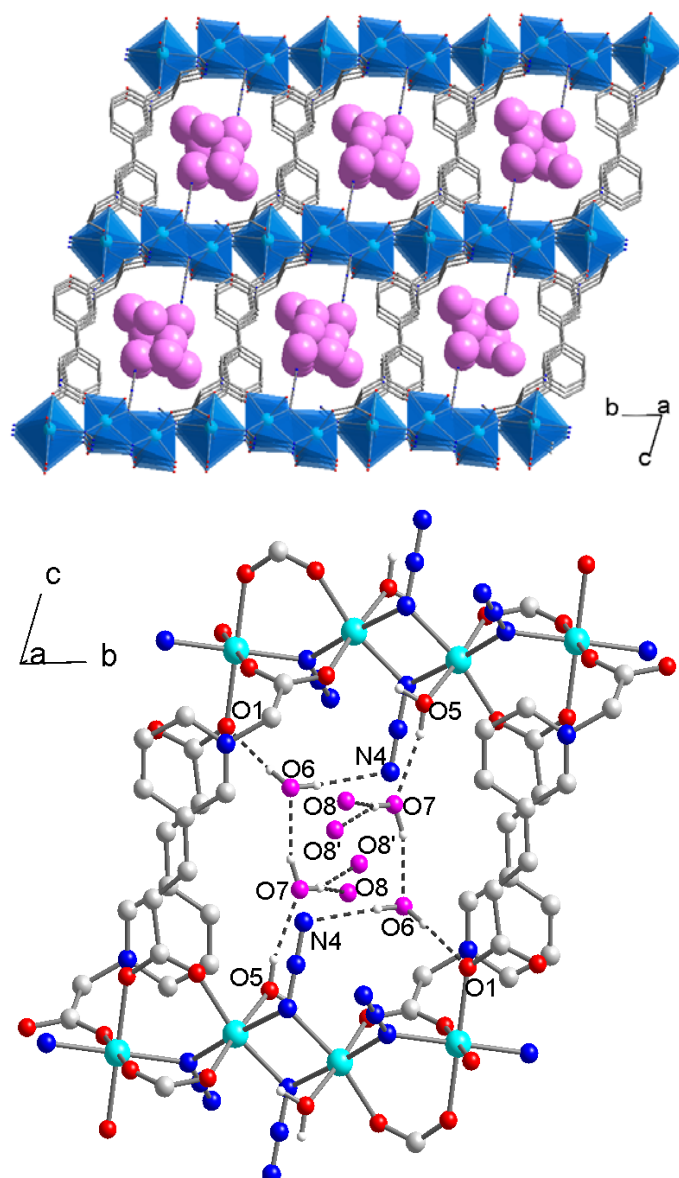


Fig. S2. Top: view of the 3D structure from the *a* direction highlighting the 1D channels and the included water molecules (large purple spheres). Bottom: view of the hydrogen bonds involving the guest water molecules (oxygens in purple; O8 and O8' are disordered). **O5-H5C...O7(-x+1, -y+1, -z):** O-H...O, 166(2)°, O...O = 2.815(6) Å, H...O = 2.01(3) Å; **O6-H6C...O1:** O-H...O, 174(4)°, O...O = 2.786(5) Å, H...O = 1.91(2) Å; **O6-H6B...N4(x, y+1, z):** O-H...N, 158(3)°, O...N = 2.94(1) Å, H...N = 2.13(4) Å; **O7-H7C...O6:** O-H...O, 162(4)°, O...O = 2.781(2) Å, H...O = 1.96(5) Å; **O7-H7B...O8:** O-H...O, 166(7)°, O...O = 2.65(2) Å, H...O = 1.78(5) Å; **O7-H7B...O8':** O-H...O, 161(7)°, O...O = 2.60(2) Å, H...O = 1.74(5) Å;

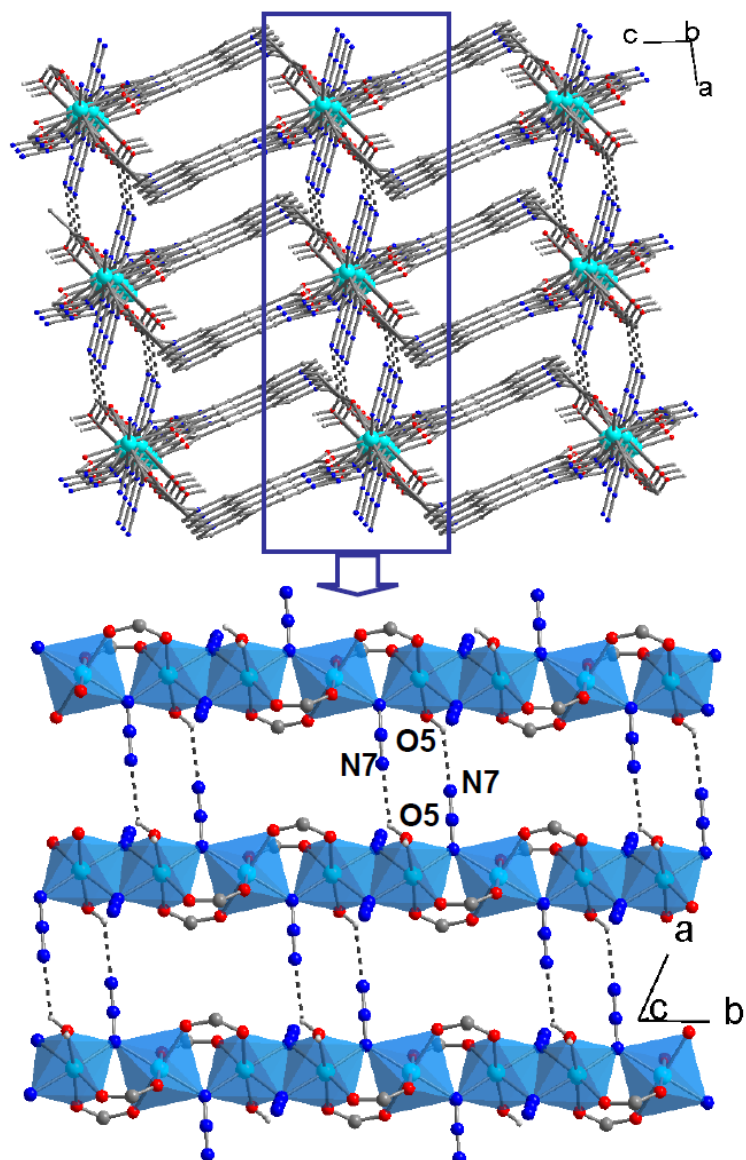


Fig. S3. Top: view of the 3D structure down the *b* direction showing the hydrogen bonds between 2D layers. Bottom: a close view showing the interlayer hydrogen bonds. O5-H...N7(-*x*+2, -*y*, -*z*+1): O-H...N = 130(2)°, O...N = 3.04(1) Å, H...N = 2.44(4) Å.

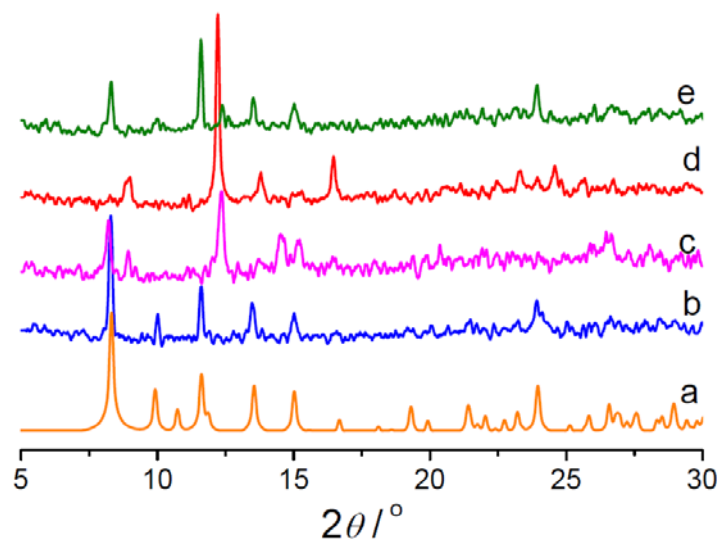


Fig. S4. Powder X-ray diffraction (PXRD) patterns: a) calculated from the crystallographic data of **1**; b) measured for **1**; c) measured for **1'**; d) measured for **2**; e) measured for **1** recovered by exposing **2** to moisture for a few days.

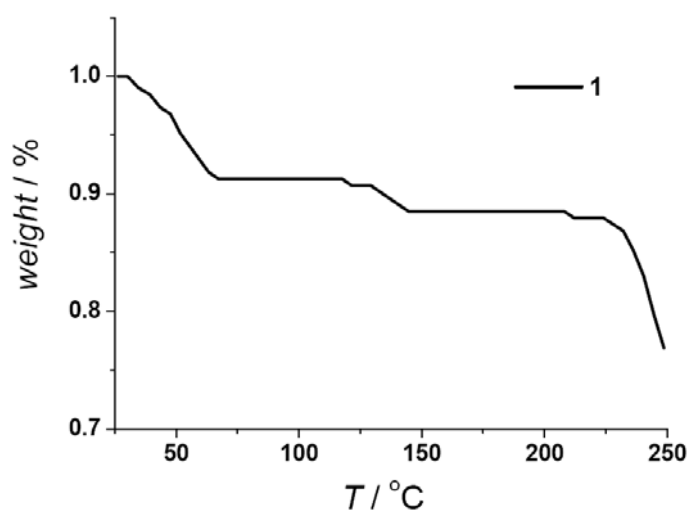


Fig. S5. The thermogravimetric curve of **1**.

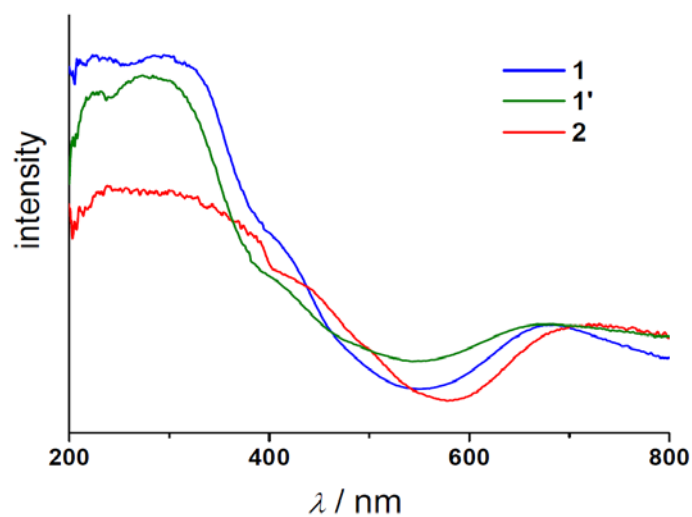


Fig. S6. Solid-state UV-vis spectra of **1**, **1'** and **2**

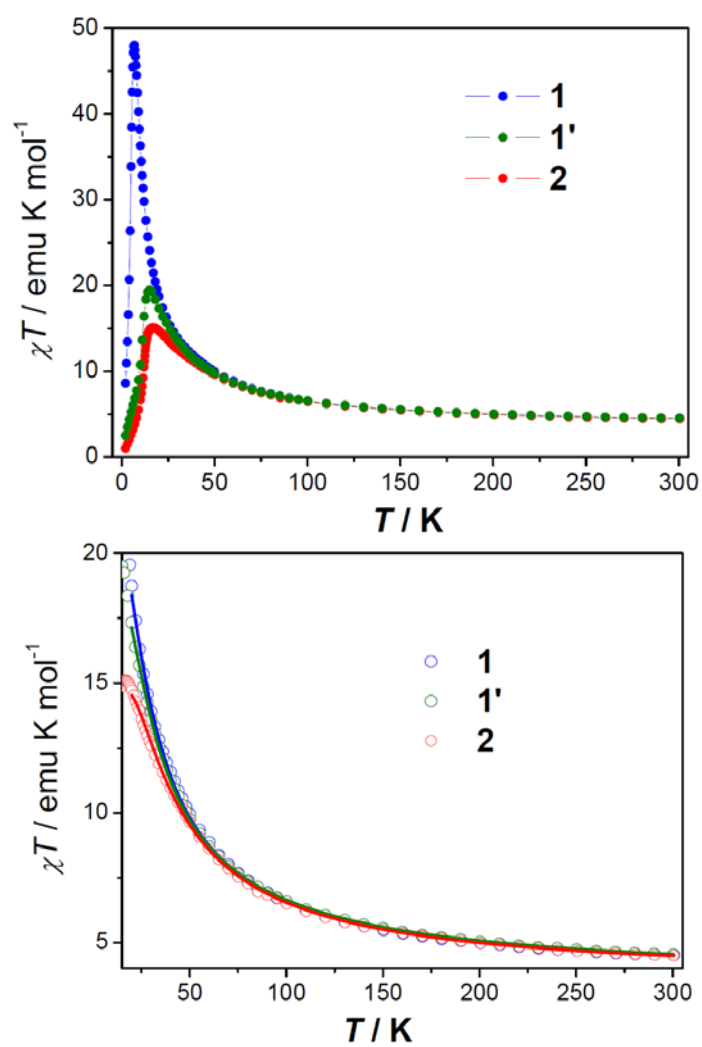


Fig. S7. Top: comparison of the χT vs T plots for **1**, **1'** and **2** at 1 kOe. Bottom: the fit (solid lines) of the data in the range 20 - 300 K (see above).

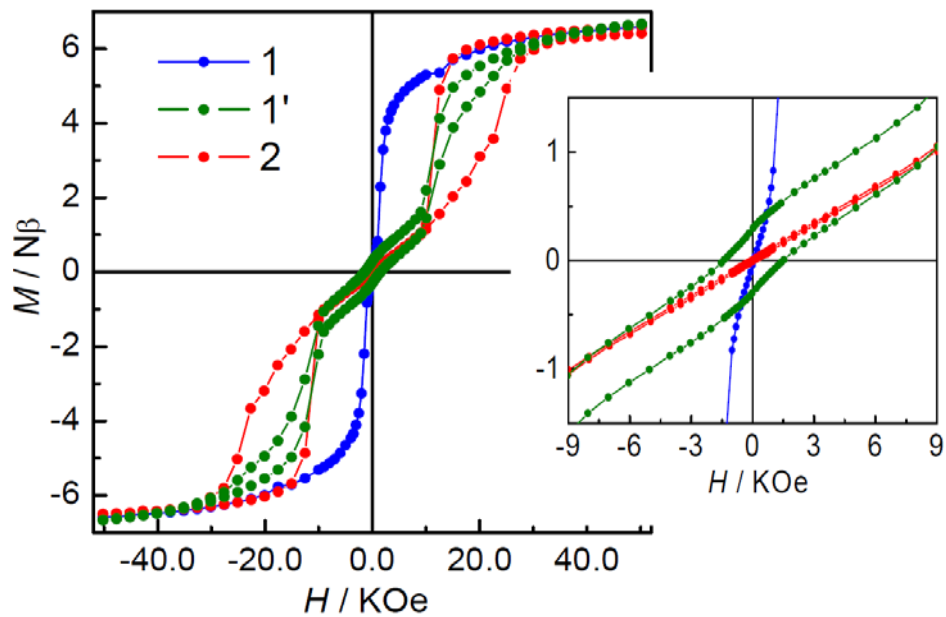


Fig. S8. Comparison of the hysteresis loops for **1**, **1'** and **2** at 2 K. The inset highlights the differences in the low field range.

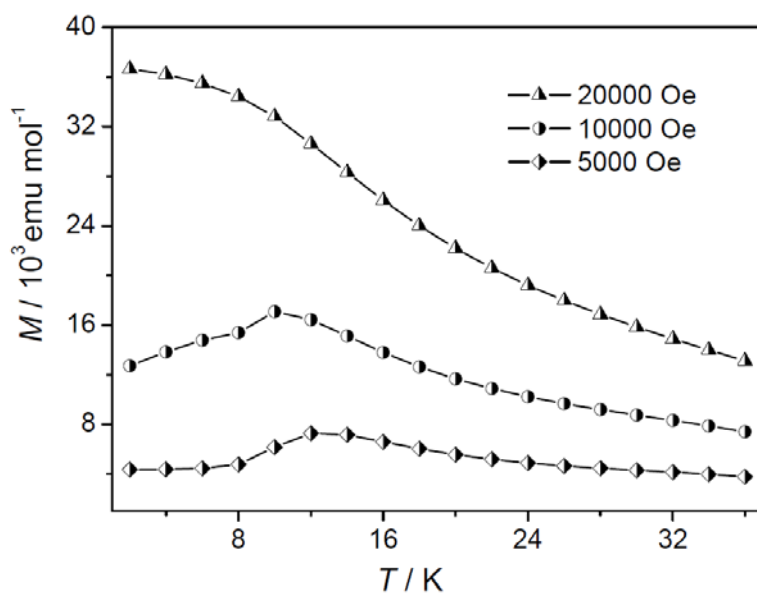


Fig. S9. Field-cooled magnetization curves for **1'** at different fields.